Biophysical Chemistry 10 (1979) 273–287

KINETICS OF TRANSPORT OF HYDROPHOBIC IONS THROUGH LIPID MEMBRANES INCLUDING DIFFUSION POLARIZATION IN THE AQUEOUS PHASE

P.C. JORDAN * and G. STARK
Fakultät für Biologie, Universität Konstanz, D-7750 Konstanz, G.F.R.

Received 25 May 1979

Previous interpretations of the kinetics of transport of hydrophobic ions through membranes have been based on one of three limiting assumptions. Either diffusion in the aqueous phase was taken to be rapid, or ionic motion was constrained to the membrane or a steady state was presumed to be established within the membrane. We present a general treatment of the coupled diffusion process through both the aqueous phase and the membrane; our theory contains the previous results as limiting cases. It is applied to voltage jump-current relaxation experiments on black lipid membranes in the presence of dipicrylamine or sodium tetraphenylborate. We have attempted to establish the rate of desorption from the membrane. For the system phosphatidylserine/tetraphenylborate, the rate of desorption and the rate of translocation were found to be comparable.

1. Introduction

The transport of lipid soluble ions through lipid bilayer membranes represents the simplest model system for the study of the permeation of hydrophobic ionic substances across biological membranes. A large number of hydrophobic ions have been found to increase the conductance of artificial lipid membranes [1,2]. The ions most extensively studied have been the dipicrylamine anion (DPA) and tetraphenylborate (TPB). Their transport mechanism has been investigated using the following methods: voltage jump [3,4], charge pulse [5], optical absorption [6], noise analysis [7] and admittance measurements [8,9]. A recent review by Andersen [10] provides a fairly complete discussion of the major results. Most experiments have been interpreted in terms of a model first suggested by Ketterer e.a. [4]. It assumes that transport proceeds by the following mechanism:

a) diffusion through the aqueous phase to the lipid membrane;
b) adsorption at the interface;
c) translocation across the membrane interior;
d) desorption into the aqueous phase;
e) diffusion in the bulk solution.

The kinetic processes b, c, and d are assumed to be first order and can be understood as a passage across activation barriers either at the interface (b and d) or within the membrane (c). This part of the transport model is illustrated in fig. 1.

Previous studies have provided estimates of the translocation rate constant k_i and the adsorption partition coefficient β. However, it has been impossible to determine k, the rate constant for desorption from the membrane. The difficulty is that the adsorption/desorption process is not readily kinetically distinguished from the aqueous diffusion process.

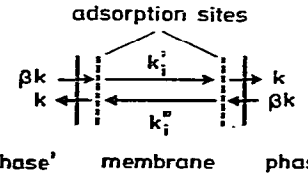

Fig. 1. Kinetic model for the transport of lipid-soluble ions through membranes [4]. Since the adsorption/desorption process is presumed to be voltage independent, the adsorption sites are at the interface.

* Permanent address: Department of Chemistry, Brandeis University, Waltham, MA. 02154, U.S.A.

The original analysis of the model under voltage jump conditions [4] was carried out assuming that the ion concentrations in the aqueous phase adjacent to the membrane remain constant for times comparable to the mean translocation time across the membrane interior. Diffusion in the aqueous phase was treated separately and assumed to be independent of the membrane translocation process. As a result both upper and lower bounds for k were obtained and it was concluded that the rate limiting step in the overall process is desorption into the aqueous phase. In fact, as was pointed out by Haydon and Hladky [11], the assumption of constant ion concentration near the interface is not generally valid. As a consequence the estimates of k are unreliable and possibly incorrect; thus the rate limiting step in the overall process has not yet been identified. The work presented here analyzes the unrestricted Ketterer model. The coupling of diffusion, adsorption and translocation processes is treated exactly. The theory is used to interpret voltage jump measurements and to provide a more reliable estimate of the desorption rate constant k.

2. Theory

2.1. Derivation of the relaxation current

Although the model will be treated in generality, it is, nevertheless, a greatly simplified representation of physical reality. The following restrictions are imposed:

1) The voltage drop occurs completely across the membrane; the electrical potential in both aqueous phases is constant. This is practically accomplished by having a large aqueous concentration of an inert electrolyte which cannot cross the membrane.

2) Only the translocation process is voltage dependent; the adsorption/desorption process is voltage independent. This is only an approximation; in fact the adsorption/desorption process is weakly voltage dependent [5,12].

3) Interactions of the hydrophobic ions within the membrane, whether they be direct (electrostatic) or indirect (via perturbation of the membrane structure) are ignored. This restricts our treatment to relatively small concentrations where saturation phenomena play no significant role [3,4,12–16].

4) The problem is treated as one dimensional, infinite in the aqueous phase, and with planar membrane surfaces. Thus we are restricted to times sufficiently short so that diffusion only occurs in the unstirred layers; as a result convection is ignored.

The constraints will be discussed at greater length in section 4.

The kinetic model is illustrated in fig. 1. When a voltage is applied, the translocation rate constant k_i is enhanced for ionic transport in one direction and reduced for motion in the opposite one; this is indicated in the figure by the two symbols k_i' and k_i''. The only charge carrier within the membrane is the lipid soluble species of valency z. The rate constant for desorption into the aqueous phase is k; that for adsorption is βk. Thus, β may be interpreted as an equilibrium constant for adsorption,

$$\beta = N/C\,, \tag{1}$$

where N is the ion surface density at the interface and C is the ionic concentration in the aqueous phase. Denoting the ion surface density in phase′ (phase″) as N' (N'') and the ionic concentrations in the two aqueous solutions as C' (C''), the equations describing the kinetic processes on the left hand side of the system (phase′) are

$$\partial C'/\partial t = D\,\partial^2 C'/\partial x^2\,, \tag{2}$$

$$\mathrm{d}N'/\mathrm{d}t = \beta k C_0' - (k + k_i')N' + k_i'' N''\,. \tag{3}$$

The analogous equations for processes occurring on the right hand side of the system are constructed by exchanging the superscripts ′ and ″. Here C_0 is the ion concentration in the aqueous solution adjacent to the adsorption layer and x is the distance from the membrane surface. In addition to the two kinetic equations, there is a boundary constraint. The flux of ions approaching the interface from the solution side is just the net rate of adsorption

$$D\,\partial C_0'/\partial x = \beta k C_0' - kN'\,, \quad x = 0\,. \tag{4}$$

The boundary condition at the right hand interface is analogous. The initial conditions are

$$C' = C'' = C\,, \quad N' = N'' = \beta C\,, \tag{5}$$

where C is the bulk concentration in the aqueous solutions. Because of the symmetry of the fundamental equations, an increase in ionic concentration a distance x from the right hand interface is balanced by the iden-

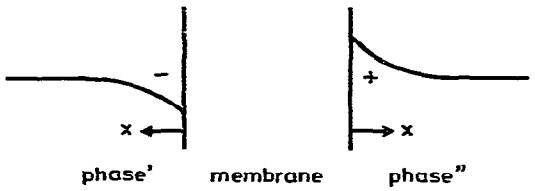

Fig. 2. Schematic concentration profile for hydrophobic anions near the membrane interface under an applied voltage.

tical decrease a distance x from the left hand interface as shown in fig. 2. Hence, we define

$$C' = C - c(x,t), \quad C'' = C + c(x,t), \tag{6}$$

$$N' = \beta C - n(t), \quad N'' = \beta C + n(t). \tag{7}$$

Substituting these equations in eqs. (2)–(4) (or their right hand side analogues) yields

$$\partial c/\partial t = D\,\partial^2 c/\partial x^2, \tag{8}$$

$$\mathrm{d}n/\mathrm{d}t = \beta k c_0 - (k + k_i' + k_i'')n + (k_i' - k_i'')\beta C, \tag{9}$$

$$D\,\partial c_0/\partial x = \beta k c_0 - kn, \quad x = 0. \tag{10}$$

In the absence of a potential difference, $k_i' = k_i''$, and the inhomogenous term in eq. (9) is zero. Under such conditions the only solution is, as it must be,

$$n(t) = c(x,t) = 0. \tag{11}$$

In general, diffusion equations can be solved using Laplace transform techniques [17]. Defining the Laplace transform

$$\bar{c}(x,s) = \int_0^\infty c(x,t)\,\mathrm{e}^{-st}\,\mathrm{d}t, \tag{12}$$

and an analogous expression for $\bar{n}(x,s)$, the Laplace transforms of eqs. (8)–(10) are

$$s\bar{c} = D\,\mathrm{d}^2\bar{c}/\mathrm{d}x^2, \tag{13}$$

$$s\bar{n} = \beta k\bar{c}_0 - (k + k_i' + k_i'')\bar{n} + (k_i' - k_i'')\beta C/s, \tag{14}$$

$$D\,\mathrm{d}\bar{c}_0/\mathrm{d}x = \beta k\bar{c}_0 - k\bar{n}, \quad x = 0, \tag{15}$$

where $\bar{c}_0 = \bar{c}(0,s)$ and the initial conditions $n(0) = c(x,0) = 0$ have been used.

As long as the system may be assumed to be infinite in extent the solution to eqs. (13) and (14), with the boundary constraint eq. (15) is

$$\bar{c}(x,s) = \frac{\bar{n}}{\beta}\frac{1}{1+q\sqrt{\omega}}\exp(-\sqrt{s/D}\,x), \tag{16}$$

$$\bar{n}(s) = \left(\frac{s}{k} + g + \frac{q\sqrt{\omega}}{1+q\sqrt{\omega}}\right)^{-1}\frac{1}{s}\frac{(k_i' - k_i'')}{k}\beta C, \tag{17}$$

$$\kappa = k_i' + k_i'', \quad q = \sqrt{sg/k}, \quad g = \kappa/k, \quad \omega = D/\kappa\beta^2. \tag{18}$$

To obtain an expression for $n(t)$, the inverse Laplace transform of eq. (17) is needed. The relevant mathematics, which requires complex variable analysis, is outlined in Appendix A. The result is

$$n(t) = \frac{\beta C(k_i' - k_i'')}{(k_i' + k_i'')} \times \left\{1 - \frac{2\sqrt{\omega}}{\pi}\int_0^\infty \frac{\exp(-u^2\kappa t)\,\mathrm{d}u}{\omega u^2[g(u^2-1)-1]^2 + (u^2-1)^2}\right\}. \tag{19}$$

The quantity of practical interest is not $n(t)$, but rather the current, $I(t)$. As we assume a single steep energy barrier, this is [4]

$$I(t) = zFA(k_i'N' - k_i''N''), \tag{20a}$$

from which, with eq. (7), we obtain

$$I(t) = zFA[(k_i' - k_i'')\beta C - (k_i' + k_i'')n(t)], \tag{20b}$$

so that, using eq. (19), one finds

$$I(t) = I_0\frac{2\sqrt{\omega}}{\pi}\int_0^\infty \frac{\exp(-u^2\kappa t)\,\mathrm{d}u}{\omega u^2[g(u^2-1)-1]^2 + (u^2-1)^2}, \tag{21}$$

$$I_0 = zFA\beta C(k_i' - k_i''), \tag{22}$$

where F is the Faraday constant and A is the area of the membrane. The integral of eq. (21) is not particularly convenient for numerical analysis. However, by determining the roots of the equation

$$\omega u^2[g(u^2-1)-1]^2 + (u^2-1)^2 = 0, \tag{23}$$

the current can be expressed in terms of the error function of complex argument, defined as

$$w(z) = \mathrm{e}^{-z^2}\,\mathrm{erfc}(-\mathrm{i}z) = \mathrm{e}^{-z^2}\left\{1 + \frac{2\mathrm{i}}{\sqrt{\pi}}\int_0^z \mathrm{e}^{-u^2}\,\mathrm{d}u\right\}, \tag{24}$$

where $\mathrm{i} = \sqrt{-1}$ and z is a general complex variable, $x + \mathrm{i}y$.

Values and properties of this function have been tabulated [18]; some of its important properties are summarized in Appendix B.

The cubic equation in u^2, eq. (23), has no positive roots. Either all three roots are negative real or one is negative real and the other two are a conjugate pair. Which of these situations obtains is determined by the values of g and ω; the distinction, as will be seen later, is physically significant. Expressing the roots of eq. (23) as $u_j^2 = -y_j$, eq. (21) may be written as

$$I(t) = \frac{I_0}{\sqrt{\omega} g^2} \sum_{j=1}^{3} \left[\frac{w(\mathrm{i}\sqrt{y_j \kappa t})}{\sqrt{y_j}} \prod_{k \neq j} \frac{1}{(y_j - y_k)} \right], \quad (25)$$

which is convenient for computation in the domain where the three quantities y_j are real and positive (the roots of the cubic equation are negative real) since then, as is clear from eq. (24), all quantities appearing in eq. (25) are real numbers. When two of the quantities y_j form a conjugate pair it is more convenient to catalog the roots of eq. (23) as

$$u_1^2 = -y_1, \quad u_2^2 = (u_3^2)^* = r\mathrm{e}^{-2\mathrm{i}\varphi}, \quad (26)$$

in which case the current is

$$I(t) = \frac{I_0/\sqrt{\omega} g^2}{y_1^2 + 2y_1 r\cos 2\varphi + r^2} \left[\frac{w(\mathrm{i}\sqrt{y, \kappa t})}{\sqrt{y_1}} + \frac{1}{r^{3/2}\sin 2\varphi} \times \{(y_1 \cos\varphi + r\cos 3\varphi)U + (y_1 \sin\varphi + r\sin 3\varphi)W\} \right], \quad (27)$$

with

$$U + \mathrm{i}W = w(\sqrt{r\kappa t}\, \mathrm{e}^{\mathrm{i}\varphi}), \quad (28)$$

all quantities appearing in eq. (27) are real. For computational purposes eqs. (25) and (27) are useful; for analytical purposes eq. (21) is sometime helpful. In only one time domain can a simple approximate expression for the current be found; as $t \to \infty$, the asymptotic approximation to $I(t)$ is easily found from eq. (21),

$$I(t) = \frac{I_0}{\beta\kappa} \sqrt{D/\pi t} \left\{ 1 + \frac{2 - \omega(1+g)^2}{2\kappa t} + \ldots \right\}, \quad (29)$$

a result only valid when both $\kappa t \gtrsim 6$ and $\kappa t \gtrsim 3\omega(1+g)^2$.

2.2. Interpretation

There are five fundamental parameters that determine the current relaxation: D, β, k, k_i' and k_i''. Of these, D is known or may be estimated with reasonable accuracy. Two relationships between the other parameters are established by the magnitude and slope of the initial current. From eqs. (9), (20) and (22) it is readily seen that

$$\kappa = k_i' + k_i'' = -(\mathrm{d}\ln I/\mathrm{d}t)_{t=0}, \quad (30a)$$

$$\beta(k_i' - k_i'') = I_0/zFCA, \quad (30b)$$

where $I_0 \equiv I(t=0)$. If the relationship between k_i' and k_i'' is known, then k_i', k_i'' and β may be established from the initial current behavior using eq. (30), as first mentioned by Haydon and Hladky [11]. Given this information the precise shape of the relaxation is determined by k. Therefore, by a comparison of theory and experiment is it in principle possible to determine k. In practice, however, k can only be obtained if it is within bounds determined by the other parameters and by the measurement accuracy.

The simplest relationship between k_i' and k_i'' is found if the membrane interior is presumed to represent a single steep and narrow energy barrier in which case [4]

$$k_i' = k_i \mathrm{e}^{zu/2}, \quad k_i'' = k_i \mathrm{e}^{-zu/2}, \quad u = VF/RT, \quad (31)$$

where V is the voltage drop across the membrane. Then, from eq. (30) we find

$$\kappa = 2k_i \cosh zu/2, \quad (32a)$$

$$I_0 = 2\beta zFACk_i \sinh zu/2. \quad (32b)$$

Thus, measurement of I_0 and $-(\mathrm{d}\ln I_0/\mathrm{d}t)$ suffice to determine β and k_i. At time sufficiently long that only the leading term of eq. (29) is significant, we find from eqs. (29)–(32),

$$I(t) = \frac{k_i' - k_i''}{k_i' + k_i''} zFCA\sqrt{D/\pi t}, \quad (33a)$$

$$= zFCA \tanh \tfrac{1}{2} zu \sqrt{D/\pi t}. \quad (33b)$$

Eq. (33b) was previously obtained by Neumcke [19] who ignored all time dependent processes within the membrane. Eq. (33a), in combination with eq. (30a), indicates that the voltage dependence of k_i' and k_i'' may be experimentally determined if measurements can be made in the domain where eqs. (29) or (33) are applicable.

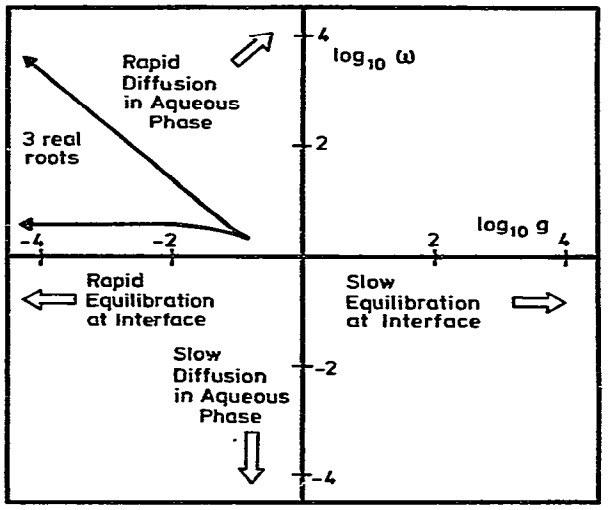

Fig. 3. Qualitative relaxation behavior in physically distinguishable domains (see text). Outside of the region with 3 real roots, eq. (23) has one real and two complex conjugate roots.

An analogous analysis has been carried out for carrier mediated transport [20].

2.2.1. Special cases

Although the final limiting current, eq. (33), is independent of k, k_i and β (the ratio $(k_i' - k_i'')/(k_i' + k_i'')$ is only a function of u), the approach to this limit is quite variable. From eq. (21) the shape of the current relaxation is determined by g and ω; depending upon the relative and absolute magnitude of these parameters qualitative differences are to be expected in the behaviour of the relaxation current. These distinctions reflect different physical possibilities, i.e. whether diffusion, adsorption/desorption, or translocation is the most significant process at relatively short times. There are four limiting domains in the $g - u$ plane illustrated in fig. 3. They are physically characterized as:

a) rapid diffusion in the aqueous phase ($g\omega \gg 1$);
b) rapid equilibration at the interface ($g \ll 1$);
c) slow diffusion in the aqueous phase ($\omega \ll 1$);
d) slow equilibration at the interface ($g \gg 1$).

To establish these assertions two of the properties of the w-function catalogued in Appendix B are of particular importance

$$w(iy) = e^{y^2}\,\mathrm{erfc}\,(y)\,, \tag{34}$$

$$U = \mathrm{Re}\,w(x) = e^{-x^2}\,. \tag{35}$$

a) *Rapid diffusion* ($\omega g = D/k\beta^2 \gg 1$). Here eq. (23) has only one real root; the values of y_1, r and φ appearing in eq. (26) are

$$y_1 = 1/\omega\gamma^2\,,\quad r = \gamma/g\,,\quad \varphi = 1/2\gamma\sqrt{\omega g\gamma}\,, \tag{36}$$

with $\gamma = g + 1$. Hence, from eq. (27) and (34), the current is

$$\frac{I(t)}{I_0} = \frac{e^{at}\,\mathrm{erfc}\,(\sqrt{at}) + gU}{1+g} + \frac{3}{2\gamma^2}\sqrt{\frac{g}{\omega\gamma}}\,W,\quad a = \frac{\kappa}{\omega\gamma^2}, \tag{37}$$

where U and W are to be calculated using eq. (28). In the limit that $\omega g \to \infty$, eq. (37) simplifies drastically. With eqs. (18), (28) and (35), the result is

$$\frac{I(t)}{I_0} = \frac{1 + g\exp\{-(k+\kappa)t\}}{1+g}\,, \tag{38}$$

precisely that of Ketterer et al. [4]. This expression is only valid at relatively short times, $t \ll a^{-1} = D\,[(k+\kappa)/k\kappa]^2$ (this time may, however, be far greater than accessible measurement times). At larger times the function $e^{at}\,\mathrm{erfc}\,(\sqrt{at})$ decreases noticeably from its initial value of 1 and eq. (38) may not be used (when $t = 0.01/a$, $e^{at}\,\mathrm{erfc}\,(\sqrt{at}) \sim 0.9$); simplification of eq. (37) is no longer possible. Until the asymptotic domain is reached each of the three terms in $I(t)$ contributes a comparable amount to the current. However, at any time the current calculated using eq. (38), i.e. when $\omega g \equiv \infty$, is an upper bound to the current in a system with the same value of g but a finite value of ωg.

b) *Rapid equilibration at the interface* ($g = \kappa/k \ll 1$). In this limit there may be either one or three real roots to eq. (23). The values of y_i are

$$y_1 = 1/\omega g^2\,, \tag{39}$$

$$(y_2, y_3) = (\omega - 2 \pm \sqrt{\omega^2 - 4\omega})/2\,, \tag{40}$$

they are real when $\omega > 4$ and y_2, y_3 form a conjugate pair when $\omega < 4$, for which

$$r = 1,\quad \varphi = \sin^{-1}(\sqrt{\omega}/2)\,. \tag{41}$$

With eqs. (25) and (27), the current, in the limit $g \to 0$, is

$$\frac{I(t)}{I_0} = U + W\tan\varphi\,,\quad U + iW = w(\sqrt{\kappa t}\,e^{i\varphi}),\ \omega < 4 \tag{42}$$

$$\frac{I(t)}{I_0} = \frac{e^s w_- - e^{-s} w_+}{e^s - e^{-s}}, \quad w_\pm = w(i\sqrt{\kappa t}\, e^{\pm s}),$$

$$s = \cosh^{-1}(\sqrt{\omega}/2), \quad \omega > 4. \tag{43}$$

When $\omega \to 0$ diffusion is relatively slow; from eq. (41) $\varphi \to 0$ and using eqs. (42) and (35), the current decay is exponential

$$I(t) = I_0 e^{-\kappa t}. \tag{44}$$

At large ω diffusion is relatively fast; from eq. (43), $s \gg 1$ and it follows, using eqs. (32) and (34), that

$$I(t) = I_0\, e^{at} \operatorname{erfc} \sqrt{at}, \quad a = \frac{1}{D}\left(\frac{I_0 \coth zu/2}{zFCA}\right)^2, \tag{45}$$

an expression identical to eq. (37) when g is small. This is equivalent to results of Neumcke [19] and of Haydon and Hladky [11]. However, the previous derivations tacitly assume that relaxation (by means of adsorption/desorption and translocation) and diffusion in the aqueous phase are independent processes that contribute additively to the current. This is not correct. Only when both interfacial equilibration and aqueous diffusion are relatively rapid processes (in the sense that $g \ll 1$ and $g\omega \gg 1$) is the current relaxation given by eq. (45). When these conditions are satisfied, the current decay depends upon only one response parameter, I_0; all other quantities are pre-assigned. For general ω in the small g domain both initial response parameter I_0 and $-(\mathrm{d} \ln I_0/\mathrm{d}t)$ are needed to determine $I(t)$. In all cases eqs. (42) and (43) (i.e. when $g = 0$) are upper bounds to the current for non-zero values of g at fixed values of ω.

c and d) *Slow diffusion in the aqueous phase* ($\omega = D/\kappa\beta^2 \ll 1$) *or slow equilibration at the interface* ($g = \kappa/k \gg 1$). When either diffusion or adsorption is relatively slow, we find the same limiting behavior for the current. This is a consequence of our assumption that only translocation kinetics are voltage dependent. A more complete analysis, including the voltage dependence of the adsorption/desorption process might distinguish between the two possibilities. In either case ions are not replenished on the left hand side of the membrane nor are they removed from the right hand side. The membrane is effectively isolated from the bulk solution. There is only one real root of eq. (23) and the values of y_1, r and φ are

$$y_1 = 1/\omega g^2, \quad r = 1, \quad \varphi = \sqrt{\omega}/2(1 + \omega g^2); \tag{46}$$

These are identical with those of eqs. (39) and (41) when g is small and to those of eq. (36) when g is large. The current, from eq. (27) is

$$\frac{I(t)}{I_0} = U + \frac{\omega^2 g^3}{(1+\omega g^2)^2}\left[e^{bt} \operatorname{erfc} \sqrt{bt} + \frac{1 + 3\omega g^2}{2(\omega g^2)^{3/2}} W\right], \quad b = \kappa/\omega g^2. \tag{47}$$

In either limit, $g \gg 1$ or $\omega \ll 1$ the second term in eq. (47) is small. For $g \to \infty$ or $\omega \to 0$, eq. (47) reduces to eq. (44); the current decays exponentially.

This of course corresponds to the most rapid decay possible; after the charges initially present on the membrane have been transferred, no further changes are possible.

2.2.2 General behavior

Depending upon the values of g and ω, the maximum current can take either the form of eq. (38) (for fixed g, as $\omega \to \infty$) or of eq. (42) or (43) (for fixed ω, as $g \to 0$). The minimum current, corresponding to the most rapid relaxation, always has the simple exponential form eq. (44). If κ and β have been established from the initial conditions via eqs. (30) and (32), then the determination of k is in practice dependent upon how substantially the maximum and minimum possible currents differ at reasonable conductance levels. It is clear that it may not always be easy to estimate k from the shape of the current function since the initial slope, eq. (30a) and the long time behavior, eq. (33), do not depend on k. The initial conditions serve only to establish $\omega = D/\kappa\beta^2$. Thus, the most direct way to determine k is by computing $I(t)/I_0$ for fixed ω at variable g. If the calculated and measured curves can be superimposed then g and, from eqs. (18) and (32), k can be obtained. To illustrate the problems with this approach, the ratio $I(t)/I_0$ is plotted as a function of g for the ω-values 10^{-4}, 10^{-2}, 1 and 10^{+2} in fig. 4. When ω is 10^{-4}, the initial slope is easily measured; however, the current is insensitive to g (and thus k) until it has fallen to below 1% of its initial value, conditions under which separation of the ionic flow from the background conductivity of the membrane becomes difficult. As ω increases, distinction between different g becomes possible. When $\omega = 10^{-2}$, finite g can be differentiated from $g = 0$ for $g \gtrsim 10$; distinction, at 2% current levels, from $g = \infty$, is still possible when $g \lesssim 100$. As ω continues to

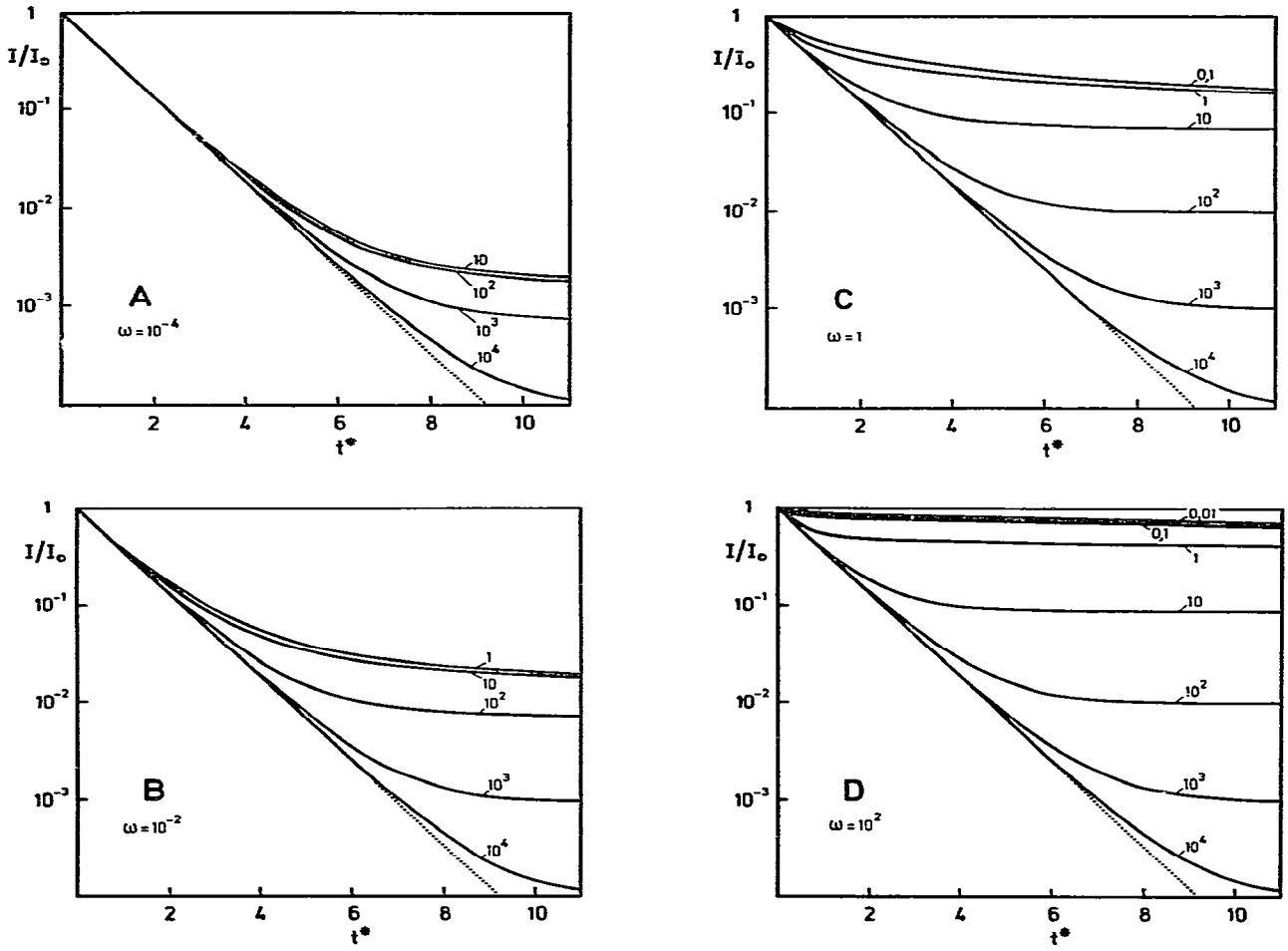

Fig. 4. Relaxation of the reduced current I/I_0 as a function of reduced time $t^* = (k_1' + k_1'')t = t/\tau$ for various values of the parameters ω and g. A) $\omega = 10^{-4}$; B) $\omega = 10^{-2}$; C) $\omega = 1$; D) $\omega = 10^2$. The values of g are given in each graph. In each case there is no noticeable change in the current relaxation if g is reduced below the smallest value given. The dashed line is the limiting reduced current when $g \to \infty$ (i.e. $k \ll k_1' + k_1''$).

increase, a different problem arises; it becomes more difficult to measure the initial slope. For $\omega = 1$ this does not appear to pose a significant problem and g can be established (again assuming the 2% current level to be accurately measurable) if it is in the range $1 \lesssim g \lesssim 100$; otherwise only bounds on g can be driven. When $\omega = 10^2$, measurements of initial slope are unreliable for $g \lesssim 0.05$ (the decrease is too small). However, for $0.05 \lesssim g \lesssim 100$ discrimination between different g is possible (again assuming that the experimental limit is the 2% current level). The general conclusions are:

a) As ω decreases, it becomes ever more difficult to establish g. If the current can be accurately followed no further than 2% of its initial value, marginal discrimination between different g is no longer possible when $\omega \lesssim 10^{-4}$.

b) As ω increases, greater discrimination is possible. Under the most favourable conditions, g may be estimated if it lies in the range $0.05 \lesssim g \lesssim 100$. If the

current can be measured more accuratley, distinction between larger values of g is possible. Otherwise only bounds on g can be determined.

One final point must be stressed. The limiting curves shown in fig. 4 represent the possible range of current values permissible with this kinetic model. Should a system exhibit a larger current than predicted, this must be interpreted as clear evidence for the inadequacy of the model.

3. Materials and methods

Relaxation experiments were made on black lipid membranes formed in unbuffered sodium chloride solutions (pH about 6) containing trace concentrations of the hydrophobic substance dipicrylamine (Fluka) and sodium tetraphenylborate (Merck). The membranes were prepared according to the technique initially described by Mueller and Rudin [2]. The lipids used were decane solutions of 1,2 dioleoyl-3-sn-phosphatidylcholine (lecithin) and phosphatidylserine isolated from ox brain. The particular method of membrane formation and the details of the voltage jump-current relaxation technique have been described previously [20,21].

Special emphasis was placed on the resolution of the current. It was measured as the voltage drop across an external resistance. The voltage was amplified by and displayed on a Tektronix oscilloscope 5115; it was then fed into a signal averager (Nicolet, model 1072) and finally plotted on an X-Y recorder. The use of signal averaging reduced the current noise considerably. Voltage pulses of variable length and amplitude were obtained from a low noise, battery driven pulse generator designed in our electronics workshop. The rest time between successive pulses was at least ten times the pulse duration; this was required in order to reestablish equilibrium. The accuracy of the current measurement depends linearly on the magnitude of the external resistance. On the other hand, by increasing this series resistance, the voltage clamp conditions across the membrane are less well approximated. As is shown in appendix C, one can correct for this effect when the applied voltage is small. For the experiments illustrated in figs. 5 and 6 we have chosen conditions where this correction is small. As a result the measurement error is greater than had we used a larger external resistance. The total external resistance is essentially composed of the measurement resistance and the solution resistance. The latter was approximated by the cell resistance without membrane (about 400 Ω in 0.1 M NaCl).

To avoid non-Ohmic effects, all measurements were carried out with an applied potential of 10 mV. The aperture used to form the membranes was 3 mm in diameter. By working with relatively large membranes and at small voltages, unwanted side effects such as electrostriction and torus effects were minimized. As measurements were made at small voltages, the slight electrode (Ag/AgCl) asymmetry potential (< 1 mV) was compensated for by introducing a variable battery driven voltage source in the external circuit. The membrane area was determined by measuring its diameter using a graticule eyepiece in conjunction with a calibrated screw micrometer. The uncertainty in the area was less than 10%.

The voltage jump apparatus and the accuracy of the current measurement was tested by using a dummy circuit (an equivalent circuit for the transport of hydrophobic ions across the membrane [4]). The error bars shown in figs. 5–7 represent the noise level, which is only significant at the lowest current levels. Calculations were performed using a PDP 11/40 computer.

4. Results and discussion

Measurements were made on four different systems; lecithin/DPA, lecithin/TPB, phosphatidylserine/DPA, and phosphatidylserine/TPB. As we have shown in section 2, the form of the current, $I(t)$, is very strongly ω-dependent. Only when $\omega \gtrsim 10^{-2}$, are there substantial deviations from exponential behavior at short times, the conditions needed to establish k. Since ω is inversibly proportional to β^2, large ω corresponds to small β. Thus by choosing membranes which possess surface charges of the same sign as the transported ions, β, the partition coefficient for adsorption, will decrease due to electrostatic repulsion *. For this reason membranes formed from negatively charged phosphatidylserine were expected to be particularly favourable. The order of magnitude of ω in 0.1 M NaCl was found to be 10^{-5} (lecithin/DPA), 10^{-3} (lecithin/TPB and phosphatidylserine/DPA) and 1 (phosphatidylserine/TPB). The

* We have defined β in terms of the aqueous bulk concentration, see eqs. (1) and (5).

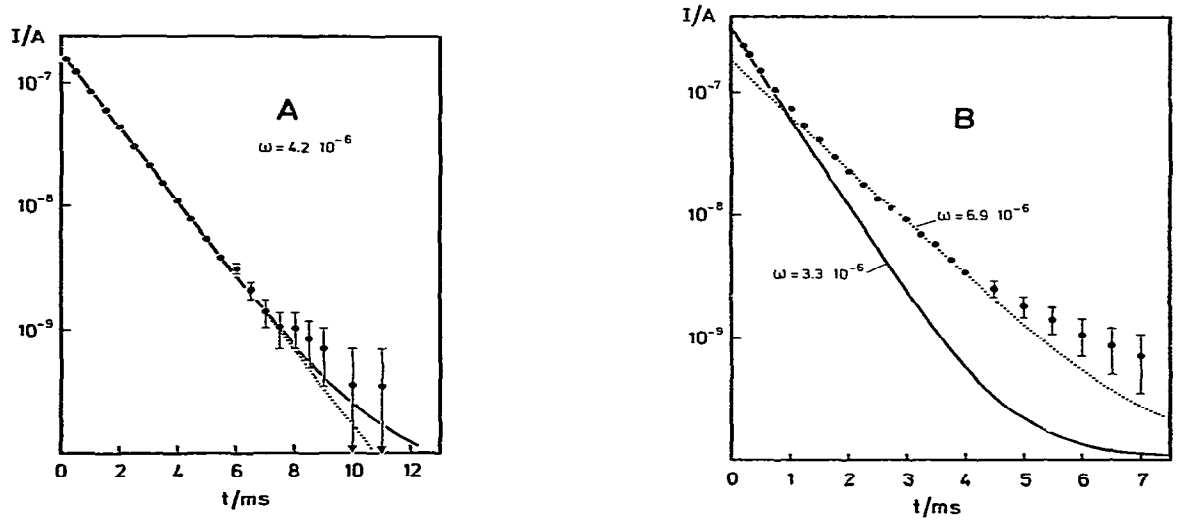

Fig. 5. Current relaxation for the system dipicrylamine/lecithin following a voltage jump of 10 mV (average of 32 pulses). The membranes were formed from a 1% solution of dioleoyllecithin in decane in the presence of 0.1 M NaCl and 5×10^{-9} M dipicrylamine in the aqueous solution (temperature 25°C). At the lower current levels the measurement uncertainty is indicated by bars. The initial current spike arising from the loading of the membrane capacity makes no significant contribution in the time range investigated (charging time about 20 μs). A) Measurement performed immediately after the membrane became black (membrane area 0.066 cm^2, measurement resistance 330 Ω, correction factor $r = 0.99$). The solid curve was calculated from eq. (27) assuming $D = 4.7 \times 10^{-6}$ cm^2 s^{-1} and using the experimental values $I_0 = 1.72 \times 10^{-7}$ A and $\kappa = 700$ s^{-1}. From these values one finds $\omega = 4.2 \times 10^{-6}$. Any value of $k \geq 2$ s^{-1} is consistent with the solid curve. The dashed curve corresponds to $k = 0$. B) Measurement performed 75 min after the blackening process (membrane area 0.072 cm^2, measurement resistance 330 Ω, correction factor $r = 0.98$). The solid curve was calculated in the same way as in A) with $I_0 = 3{,}25 \times 10^{-7}$A, $\kappa = 1676$ s^{-1} and $k \geq 4$ s^{-1} ($\omega = 3.3 \times 10^{-6}$). The dashed line was obtained assuming $I_0 = 1.75 \times 10^{-7}$ A, $\kappa = 1012$ s^{-1} and $k \geq 3$ s^{-1} ($\omega = 6.9 \times 10^{-6}$) (see text).

diffusion coefficients used were 5.2×10^{-6} cm^2 s^{-1} (TPB) (22) and 4.7×10^{-6} cm^2 s^{-1} (DPA); the latter was estimated from the value for TPB assuming Stokes' law. Of the four systems investigated, the results obtained for three cases are presented in detail.

In figs. 5, 6 and 7 the results of typical experiments are illustrated. Fig. 5 pertains to a system which has been frequently studied using relaxation techniques — a neutral membrane doped with DPA [4–6,14]. In this case, as in the analogous TPB system [4,5,12,15], exponential current decrease over many relaxation times (at least at low concentrations) has been reported. This observation was only confirmed for measurements made with membranes shortly after they became black (fig. 5A). As the membranes aged, the relaxation became clearly non-exponential, even at short times (fig. 5B). A similar effect, as membranes aged, was observed with the lecithin/TPB system. For phosphatidylserine membranes (fig. 6) this aging effect could not be studied since the blackening process was very slow so that only aged membranes were investigated. A possible interpretation of this effect is presented later.

Before analysing the experimental data using the theory developed in section 2, we wish to rule out a possible source of systematic error. Under ideal voltage jump conditions, the total drop of the applied voltage occurs across the membrane. In reality, the circuit acts as a series resistance. The voltage is partitioned among the membrane resistance R_M, the resistance of the aqueous solution R_S, and the measurement resistor R_A. Under the experimental conditions used, $R_A + R_S$ was a small fraction of R_M (always less than 5%, usually less than 2%). Thus, the voltage drop across the membrane is weakly time dependent. In general this alters the mathematical properties of the equations used to describe the problems; as a result the analytical form of the current function, $I(t)$, depends on the series resistance $R_E \equiv R_A + R_S$ and eq. (21) would not be applicable. However, this difficulty is circumvented if we restrict ourselves to small voltages (the Ohmic range of

the membrane). As shown in Appendix C, eq. (21) is then still correct. The only difference is that the translocation rate constant k_i is to be replaced by $k_i r$, where $r = 1 - R_E/(R_E + R_M(t=0))$; $R_M(t=0)$ is the initial membrane resistance. As long as the restriction to the Ohmic domain is satisfied, the functional form of $I(t)$, eq. (21), remains unaltered. Under our experimental conditions this effect negligibly alters k_i (less than 3%).

Another difficulty arises because the adsorption/desorption process is weakly voltage dependent [12]. Our model ignores this complication; the consequence of this simplification will be discussed later. One point must be stressed now. This effect provides another source for deviation from ideal voltage clamp conditions and leads to a distortion of the analytical form of the current function, $I(t)$ [15,16]. As long as the applied voltage is small, there is no alteration in the analytical form of $I(t)$. This follows using arguments analogous to those presented in Appendix C. It has previously been demonstrated for systems where diffusion plays no role, i.e. strict exponential decay [16]. There is, however, a change in the initial value of the slope of $\log I(t)$. The magnitude of this change is proportional to the concentration of the transported ions in the membrane. As in our experiments the ion concentration in the membrane is small enough (with the possible exception of the experiment illustrated in fig. 7), this effect should not be important [15,16]. In summary, the experimental conditions, i.e. concentration range, voltage and external resistance ($R_S + R_A$) were chosen so that ideal voltage clamp conditions were very well approximated.

We shall now proceed to our method of data analysis. As already mentioned I_0 and $\kappa = (-\mathrm{d} \ln I_0/\mathrm{d}t)$ are obtained from the initial time dependence of the current. With these values ω is calculated using eqs. (18), (22) and (31)

$$\omega = (zFC \tanh zu/2)^2 (A^2 D \kappa / I_0^2) . \qquad (48)$$

Then $I(t)/I_0$ is calculated from eq. (25) or (27) for various g and compared with the experimental data. From the best fit of theory and experiments, g and, using eq. (18), k are obtained.

For the system lecithin/DPA there is good agreement between theory and experiment for measurements made on recently formed membranes (fig. 5A). There appears to be a distinct curvature in $\ln I(t)$; this could be accounted for by the solid curve, corresponding to the limiting case $k \gtrsim 2\ \mathrm{s}^{-1}$. However, the experimental uncertainties at long times are large enough that one cannot rule out the dashed curve, corresponding to the limiting case $k = 0\ \mathrm{s}^{-1}$. This is a consequence of the very small ω value.

Surprisingly, theory and experiment cannot be brought into agreement when measurements are made using aged membranes. The data presented in fig. 5B are typical. When the initial values of the current and its slope are used to calculated $I(t)/I_0$, there are enormous discrepancies between theory and experiment. Until 4 ms the experimental $I(t)$ can be accounted for by a sum of two exponential relaxations; the theory, of course, only predicts one. Even if we use the *ad hoc* procedure of assuming that the slow relaxation corresponds to the processes we have treated theoretically (the dashed curve in fig. 5B), there remains a discrepancy. The reason for this difference is unknown. One possible cause is the voltage dependence of the adsorption/desorption process, already mentioned in another context. We have not included this dependence in our analysis because of the enormous increase in computational complexity that would ensue. However, as we could show, when this effect is accounted for, the form of the function describing the short time current decay is altered; in addition, when diffusion is very fast, the function describing the short time current decay must be replaced by the sum of two exponential functions (unpublished). Thus it is conceivable that a more complete theory, also treating the voltage dependence of the adsorption/desorption process, would account for experiments such as that presented in fig. 5B. On the other hand this phenomenon should also be present when the membranes are fresh; however, there is no hint of deviation from exponential behavior in the short time domain in fig. 5A ($t \lesssim 5$ ms). This could be rationalized if the surface process is less important in freshly prepared membranes. It is well known that the specific membrane capacitance increases as membranes age [24], indicating that the membranes become thinner, conditions under which surface effects should be more significant. We do not presently know whether these phenomena are sufficient to account for the anomalies. Other effects such as a time dependent increase of the unspecific background conductivity might also contribute.

The phosphatidylserine/TPB system, illustrated in fig. 6, shows the effect of relatively large ω ($\omega \approx 1$). There is no clearly defined domain of exponential decay

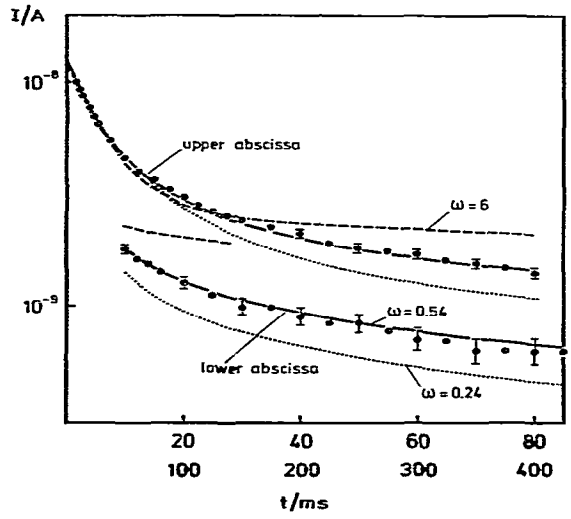

Fig. 6. Current relaxation for the system tetraphenylborate/serine following a voltage jump of 10 mV (average of 8 pulses). The membrane was formed from a 0.2% solution of phosphatidylserine in decane in the presence of 0.1 M NaCl and 10^{-6} M sodium tetraphenylborate in the aqueous solution (temperature 25° C, membrane area 0.061 cm^2, measurement resistance 3.3 kΩ, correction factor $r = 0.995$). At the lower current levels the measurement uncertainty is indicated. The initial current spike does not contribute in the time range considered (charging time about 100 μs). All curves were calculated using $D = 5.2 \times 10^{-6}$ cm^2 s^{-1}, $I_0 = 1.2 \times 10^{-8}$ A and $\kappa = 133$ s^{-1}. The solid curve was obtained asusming $C = 3 \times 10^{-7}$ M ($\omega = 0.54$) and $k = 79$ s^{-1}, the dashed curve assuming $C = 10^{-6}$ M ($\omega = 6$) and $k = 41$ s^{-1} and the dotted curve assuming $C = 2 \times 10^{-7}$ M ($\omega = 0.24$) and $k = 133$ s^{-1} (see text for details).

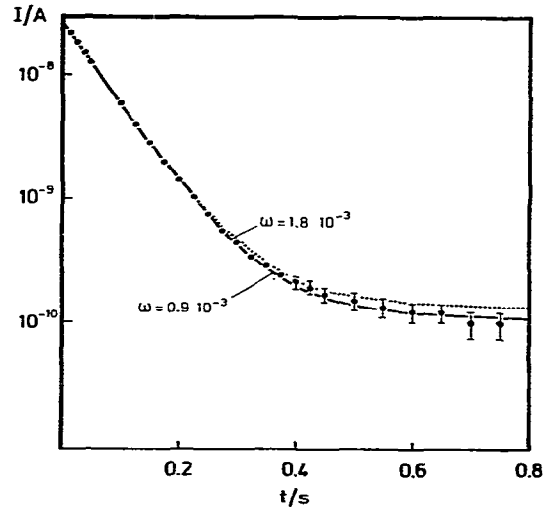

Fig. 7. Current relaxation for the system tetraphenylborate/lecithin following a voltage jump of 10 mV (average of 8 pulses). The membrane was formed from a 0.5% solution of dioleoyllecithin in decane in the presence of 0.1 M NaCl and 10^{-7} M sodium tetraphenylborate in the aqueous solution (temperature 25° C, membrane area 0.069 cm^2, measurement resistance 10 kΩ, correction factor $r = 0.97$). At the lower current levels the measurement uncertainty is indicated. The initial current spike does not contribute in the time range considered (charging time about 250 μs). Measurements were made 10 min after the membrane became black. Both curves were calculated using $D = 5.2 \times 10^{-6}$ cm^2 s^{-1}, $I_0 = 2.7 \times 10^{-8}$ A and $\kappa = 15.2$ s^{-1}. The solid curve was obtained assuming $C = 7 \times 10^{-8}$ M ($\omega = 0.9 \times 10^{-3}$) and $k = 0.15$ s^{-1}, the dashed curve assuming $C = 10^{-7}$ M ($\omega = 1.8 \times 10^{-3}$) and $k = 0.15$ s^{-1}.

in agreement with the theory for smaller g values (see fig. 4c). As already mentioned in section 2.2.2, these are the most favourable conditions for estimating k. As the membrane is negatively charged, the aqueous anion concentration directly at the membrane interface is much less than the bulk anion concentration. The concentration change occurs within approximately one Debye length (10 Å with ionic strength 0.1 M). The time required for diffusion in either direction through such a short distance is many orders of magnitude less than the times relevant in our analysis. Thus, this phenomenon has no bearing on the determination of k.

In order to obtain a good fit of theory and experiment we had to assume that the bulk concentration of TPB at the time of measurement was less than the concentration initially present when the membrane was formed. As mentioned previously, the time required for the blackening process to be completed is quite long for these systems (normally ~1 hour). This is long enough so that a substantial fraction of the TPB, originally in the aqueous phase, can be leached out into the torus containing the membrane forming solution. In the experiment illustrated the best fit was found assuming $C = 3 \times 10^{-7}$ M, 30% of the concentration initially present. For the other four membranes studied the concentration decrease was not as extreme as that shown here. Though not studied exhaustively we found that there was a direct correlation between the age of the membrane and the decrease in the concentration**. As pointed out in fig. 6 the value of k is not very sen-

** For footnote see next page.

sitive to the choice of C. The numerical value of k is even less affected by small errors in the determination of the membrane area and slight uncertainties in the value of D. There remains a definite uncertainty in the determination of k, since we have ignored the voltage dependence of the adsorption/desorption process. Though the voltage dependence is probably very small [15], we cannot, within the framework of our theory, estimate how this would be reflected in the numerical value of k. If one accepts our value of k, then the rate of the desorption process is comparable to the rate of translocation, at least for the phosphatidylserine/TPB system.

For the other systems studied, the estimation of k is much more difficult even though there is good agreement between theory and experiments made with relatively young membranes. Fig. 7 illustrates this for the tetraphenylborate/lecithin system. In order to account for the data at long times, it was necessary to assume $C = 7 \times 10^{-8}$ M, 80% of the amount initially present. In spite of the good fit, it should be pointed out that the difference between $I(t)$ calculated for $k = 0.15\ s^{-1}$ and $k \to \infty$ ($k \geq 0.6\ s^{-1}$) is small, although experimentally significant (not shown in the figure). Because the difference is small, we cannot rule out that refining the kinetic model (e.g. by introducing the voltage dependence of the adsorption/desorption process) would appreciably modify the value of k for this system.

In general, to determine k when ω is small (i.e. aqueous diffusion a relatively slow process) there are two major experimental obstacles. First, great precision is required in the current measurement; this can be accomplished by using a large measurement resistance R_A. Such experiments, which increase the importance of the correction factor r (see Appendix C), have been carried out on all the systems investigated here. This is of no particular benefit, because the concentration of the transported ions in the aqueous solution is not known with accuracy as ions are continually being leached into the torus surrounding the membrane. To establish k, when ω is small, an independent measurement of the ionic concentration is desirable. Fortunately, when ω is large, the concentration can be established indirectly from the current at long times (see fig. 6). For the small ω domain, other experimental approaches, such as the temperature jump technique (work in progress), may provide more favourable conditions for estimation of k.

** We cannot rule out the possibility that there is a similar concentration decrease under the experimental conditions illustrated in fig. 5B. If such an effect were present and were accounted for, the discrepancies between theory and experiment would be even greater.

Acknowledgements

We wish to thank K. Janko of our laboratory for preparation of the lipids. This research has been supported by the Deutsche Forschungsgemeinschaft (Sonderforschungsbereich 138). One of us (PCJ) wishes to thank the Whiting Foundation for fellowship support; he also wishes to express his gratitude to Prof. P. Läuger and all members of the membrane biophysics group for their hospitality.

Appendix A

Inverse Laplace transformation of $\bar{n}(s)$

The inverse Laplace transform of $\bar{n}(s)$ is

$$n(t) = \frac{1}{2\pi i}\int_{b-i\infty}^{b+i\infty} e^{st}\,\bar{n}(s)\,ds\,, \qquad (A.1)$$

where b is chosen so that the path of integration in the complex s-plane is to the right of all singularities of $\bar{n}(s)$ [25]. According to a fundamental theorem of complex variable analysis, the integral around any closed contour on which the integrand is continuous can be calculated from the limiting properties of the integrand at any poles inside the contour [26]; if there are no such points the integral around the closed path is zero. Consider the contour shown in fig. 8. The quantity e^{st} is everywhere finite. The denominator of $\bar{n}(s)$ from eq. (17) is

$$s\left\{\frac{s}{k} + g + \frac{\sqrt{g\omega s/k}}{1+\sqrt{g\omega s/k}}\right\}, \qquad (A.2)$$

so that poles of $\bar{n}(s)$ are determined by the zeros of this function. Since the point $s = 0$ is exterior to the contour, only the zeros of the quantity in braces need be considered. Defining

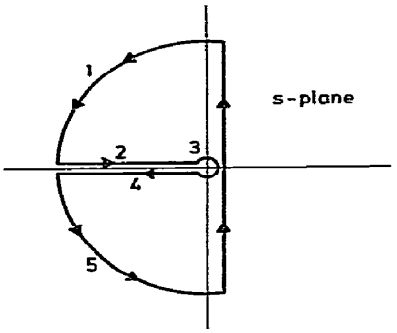

Fig. 8. Integration contour for computing the inverse Laplace transform of $\bar{n}(s)$.

$$g\omega s/k = R^2 e^{2i\varphi}, \quad R>0, \ -\pi/2<\varphi<\pi/2, \tag{A.3}$$

the factor in braces is

$$\frac{1}{g\omega} R^2 e^{2i\varphi} + g + \frac{R e^{i\varphi}}{1+R e^{i\varphi}} \equiv Q, \tag{A.4}$$

from which we find

$$\mathrm{Re}\, Q = \frac{1}{g\omega} R^2 \cos 2\varphi + g + \frac{R\cos\varphi + R^2}{1+R^2+2R\cos\varphi}, \tag{A.5}$$

$$\mathrm{Im}\, Q = R\sin\varphi \left\{ \frac{2R\cos\varphi}{g\omega} + \frac{1}{1+R^2+2R\cos\varphi} \right\}. \tag{A.6}$$

Q is zero only if $\mathrm{Re}\, Q$ and $\mathrm{Im}\, Q$ are simultaneously zero. Since $|\varphi| < \pi/2$ it is clear that only when $\varphi = 0$ can $\mathrm{Im}\, Q$ be zero. However, when $\varphi = 0$

$$\mathrm{Re}\, Q = R^2/g\omega + g + R/(1+R) > 0, \tag{A.7}$$

since $R > 0$. Thus $\bar{n}(s)$ has no poles inside the designated contour and so the integral along that path is zero. However, $\bar{n}(s)$ does have an important singularity reflected in the way the contour was chosen. It is discontinuous across the negative real axis; from eq. (A.6)

$$\mathrm{Im}\, Q = \pm R/(1+R^2), \quad \varphi \to \pm\pi/2. \tag{A.8}$$

The integral eq. (A.1) is equal to the sum

$$n(t) = -\sum_{j=1}^{5} f_j(t), \tag{A.9}$$

where $f_j(t)$ indicates the integral of $e^{st}\bar{n}(s)/2\pi i$ along segment j in fig. 8. Along segments (1) and (5), $e^{st} \to 0$ as $s \to \infty$; thus only segments (2)–(4) need be considered. Defining

$$\begin{aligned} s &= u^2\kappa e^{\pi i} && \text{segment (2)} && \infty > u > 0, \\ s &= \kappa\epsilon e^{\varphi i} && \text{segment (3)} && \pi > \varphi > -\pi, \\ s &= u^2\kappa e^{-\pi i} && \text{segment (4)} && 0 < u < \infty, \end{aligned} \tag{A.10}$$

and using eq. (A.1), (A.9), (17) and (18), the non-zero contributions to eq. (A.9) are

$$\begin{aligned} f_2(t) &= \frac{n_\infty}{2\pi i} \int_{\infty}^{0} \frac{2\,du}{u} \frac{\exp(-u^2\kappa t)}{g} \\ &\quad \times \left\{ -u^2 + 1 + \frac{i\sqrt{\omega}u}{1+ig\sqrt{\omega}u} \right\}^{-1}, \\ f_3(t) &= \frac{n_\infty}{2\pi i} \int_{\pi}^{-\pi} i\,d\varphi \frac{\exp(\epsilon\kappa t e^{i\varphi})}{g} \\ &\quad \times \left\{ \epsilon e^{i\varphi} + 1 + \frac{i\sqrt{\omega}\sqrt{\epsilon}\, e^{i\varphi/2}}{1+ig\sqrt{\omega}\sqrt{\epsilon}\, e^{i\varphi/2}} \right\}^{-1}, \\ f_4(t) &= f_2^*(t) = \frac{n_\infty}{2\pi i} \int_{0}^{\infty} \frac{2\,du}{u} \frac{\exp(-u^2\kappa t)}{g} \\ &\quad \times \left\{ -u^2 + 1 - \frac{i\sqrt{\omega}u}{1-ig\sqrt{\omega}u} \right\}^{-1}, \end{aligned} \tag{A.11}$$

with $n_\infty = (k_i' - k_i'')\beta C/k$. Summing $f_2(t)$ and $f_4(t)$, letting $\epsilon \to 0$ in $f_3(t)$ and substituting in eq. (A.9) leads immediately to eq. (19).

Appendix B

Properties of w(z)

The function $w(z)$ is defined as

$$w(z) = e^{-z^2} \left\{ 1 + \frac{2i}{\sqrt{\pi}} \int_0^z dt\, e^{t^2} \right\}. \tag{B.1}$$

For real z ($z = x$)

$$w(x) = e^{-x^2} + i\frac{2}{\sqrt{\pi}} e^{-x^2} \int_0^x dt\, e^{t^2}, \tag{B.2}$$

for imaginary z ($z = iy$)

$$w(\mathrm{i}y) = \mathrm{e}^{y^2}\left\{1 - \frac{2}{\sqrt{\pi}}\int_0^y \mathrm{d}t\,\mathrm{e}^{-t^2}\right\} = \mathrm{e}^{y^2}\,\mathrm{erfc}\,(y)\,. \tag{B.3}$$

The function has the fundamental property, easily established from eqs. (B.1) and (B.2),

$$w(-x+\mathrm{i}y) = w^*(x+\mathrm{i}y)\,, \tag{B.4}$$

where w^* is the complex conjugate of w. Tabulations of $w(z)$ exist (18); however, they are not convenient for most computational purposes.

Defining

$$\varphi = \tan^{-1}(x/y)\,, \quad T = x^2+y^2\,, \tag{B.5}$$

$$S = \sin 2\varphi, \quad C = \cos 2\varphi\,, \tag{B.6}$$

$$\xi = TS\,, \quad \gamma = \xi - \varphi\,, \tag{B.7}$$

$w(z)$ can be written as

$$w(z) = \mathrm{e}^{-TC}\{\cos\xi + A\sin\gamma - B\cos\gamma\} + \mathrm{i}\mathrm{e}^{-TC}\{-\sin\xi + A\cos\gamma + B\sin\gamma\}\,, \tag{B.8}$$

where

$$A = \frac{1}{\sqrt{\pi}}\int_0^T \frac{\mathrm{d}t}{\sqrt{t}}\mathrm{e}^{tC}\cos tS\,, \quad B = \frac{1}{\sqrt{\pi}}\int_0^T \frac{\mathrm{d}t}{\sqrt{t}}\mathrm{e}^{tC}\sin tS\,. \tag{B.9}$$

As long as $T \leqslant 1$ the integrals A and B may be quickly calculated by using the series expansion

$$A = \frac{2R}{\sqrt{\pi}}\sum_{n=0}^{\infty}\frac{T^n\cos 2n\varphi}{(2n+1)n!}\,, \quad B = \frac{2R}{\sqrt{\pi}}\sum_{n=0}^{\infty}\frac{T^n\sin 2n\varphi}{(2n+1)n!}\,. \tag{B.10}$$

When $T > 1$ and $TC > -1$, A and B are computed from eq. (B.9) using the series expansion (in the domain $t \leqslant 1$) and using gaussian quadratures (in the domain $t > 1$).

When $C < 0$, $w(z)$ may be expressed as

$$w(z) = \{-\tilde{A}\sin\gamma + \tilde{B}\cos\gamma\} - \mathrm{i}\{\tilde{A}\cos\gamma + \tilde{B}\sin\gamma\}\,, \tag{B.11}$$

where

$$\tilde{A} = \frac{1}{\sqrt{\pi}}\int_T^{\infty}\frac{\mathrm{d}t}{\sqrt{t}}\mathrm{e}^{C(t-T)} = \frac{1}{\sqrt{\pi|C|}}\int_0^{\infty}\mathrm{d}y\,\mathrm{e}^{-y}\,\frac{\cos(y\,s/|C| + T)}{\sqrt{y+T|C|}}\,. \tag{B.12}$$

The expressions for B are analogous with sines replacing cosines. Numerical evaluation of eq. (B.12) is quickly accomplished using Laguerre quadratures as long as $T|C| > 1$. Eq. (B.11) is *only* valid when $C < 0$; it is a practical improvement over eq. (B.8) when $TC < -1$. When $x > 3.9$ or $y > 3.0$, $w(z)$ may be computed directly using the rational approximations [18]

$$w(z) = \mathrm{i}z\left\{\frac{0.4613135}{z^2-0.1901635} + \frac{0.09999216}{z^2-1.7844927} + \frac{0.002883894}{z^2-5.5253437}\right\}, \tag{B.13}$$

or when $x > 6$ or $y > 6$

$$w(z) = \mathrm{i}z\left\{\frac{0.5124242}{z^2-0.2752551} + \frac{0.05176536}{z^2-2.724745}\right\}. \tag{B.14}$$

Appendix C

Correction for non-ideal voltage clamp

Under voltage clamp conditions, the total potential drop is

$$V = I(R_{\mathrm{E}} + R_{\mathrm{M}})\,; \tag{C.1}$$

of this the quantity $U = R_{\mathrm{M}}I$ is the voltage drop across the membrane. $R_{\mathrm{E}} = R_{\mathrm{A}} + R_{\mathrm{S}}$ is the total series resistance. It is this unknown voltage which governs the ionic transport. Combining eqs. (C.1), (20) and (31) we find the following expression for U

$$(V-U)/R_{\mathrm{E}} = 2zFA\,k_{\mathrm{i}}[\beta C\sinh zu/2 - n(t)\cosh zu/2]\,, \tag{C.2}$$

with $u = FU/RT$. In general, no closed form solution of eq. (C.2) for U is possible. However, when u is small $\sinh zu/2 \sim zu/2$ and $\cosh zu/2 \sim 1$; the solution of eq. (C.2) is then

$$u = (v + 2bn(t)), \quad v = FV/RT\,, \tag{C.3a}$$

$$b = k_{\mathrm{i}}zR_{\mathrm{E}}(F^2/RT), \; r = (1+bzA\beta C)^{-1}\,. \tag{C.3b}$$

Of the equations which describe our model, eqs. (8-10), only eq. (9) depends explicitly on u. Substituting eq. (C.3a) in eq. (9), using eq. (31), and restricting ourselves to the small u region, we find

$$\mathrm{d}n/\mathrm{d}t = \beta k c_0 - (k + 2k_{\mathrm{i}}r)n + k_{\mathrm{i}}rz\beta C v\,. \tag{C.4}$$

Comparing this expression with eq. (9) it is only necessary to replace k_i by $k_i r$, as long as we restrict ourselves to small voltages. The same replacement (k_i by $k_i r$) is required for the initial current eq. (22). Thus we have the identifications

$$\kappa = 2k_i r\,, \quad \text{(instead of } k_i' + k_i''\text{)}\,, \tag{C.5a}$$

$$I_0 = zFA\beta Ck_i \upsilon r\,,$$

$$\text{(instead of } zFA\beta C(k_i' - k_i'')\text{)}\,. \tag{C.5b}$$

The correction factor r can be calculated by rewriting eq. (C.5b) as

$$zA\beta C = I_0/(Fk_i \upsilon r)\,, \tag{C.6}$$

and substituting this in eq. (C.3b). We obtain, with eq. (C.1)

$$r = 1 - \frac{bI_0}{zFk_i\upsilon} = 1 - \frac{I_0 R_E}{V} = 1 - \frac{R_E}{R_E + R_M(t=0)}\,, \tag{C.7}$$

where $R_M(t=0)$ is the initial membrane resistance.

References

[1] Y.A. Liberman and V.P. Topaly, Biofizika 14 (1969) 452.
[2] P. Mueller and D.O. Rudin, in: Current topics in bioenergetics, Vol. 3, ed. D.R. Sanadi (Academic Press, New York, 1969) p. 157.
[3] O.H. LeBlanc, Jr., Biochim. Biophys. Acta 193 (1969) 350.
[4] B. Ketterer, B. Neumeck and P. Läuger, J. Membrane Biol. 5 (1971) 225.
[5] R. Benz, P. Läuger and K. Janko, Biochim. Biophys. Acta 455 (1976) 701.
[6] J. Wulf, R. Benz and W.G. Pohl, Biochim. Biophys. Acta 465 (1977) 429.
[7] H.-A. Kolb and P. Läuger, J. Membrane Biol. 37 (1977) 321.
[8] R. De Levie, N.G. Seidah and D. Larkin, Electroanal. Chem. Interfac. Electrochem. 49 (1974) 153.
[9] R. De Levie and D. Vukadin, Electroanal. Chem. Interfac. Electrochem. 62 (1975) 95.
[10] O.S. Andersen, in: Membrane transport in biology, Vol. I, eds. G. Giebisch, D.C. Tosteson and H.H. Ussing (Springer, Berlin, 1978) p. 369.
[11] D.A. Haydon and S.B. Hladky, Quart. Rev. Biophys. 5 (1972) 187.
[12] O.S. Andersen and M. Fuchs, Biophys. J. 15 (1975) 795.
[13] L.J. Bruner, Biophysik 6 (1970) 241.
[14] L.J. Bruner, J. Membrane Biol. 22 (1975) 125.
[15] O.S. Andersen, S. Feldberg, H. Nakadomari, S. Levy and S. McLaughlin, Biophys. J. 21 (1978) 35.
[16] S.W. Feldberg and A.B. Delgado, Biophys. J. 21 (1978) 71.
[17] H.S. Carslaw and J.C. Jaeger, Conductance of heat in solids (University Press, Oxford, 1959) p. 297.
[18] M. Abramowitz and I.A. Stegun, Handbook of Mathematical Functions (Dover Publ. N.Y., 1965) p. 297.
[19] B. Neumcke, Biophysik 7 (1971) 95.
[20] W. Knoll and G. Stark, J. Membrane Biol. 25 (1975) 249.
[21] G.W. Pohl, W. Knoll, B.F. Gisin and G. Stark, Biophys. Struct. Mech. 2 (1976) 119.
[22] J.F. Skinner and R.M. Fuoss, J. Phys. Chem. 68 (1964) 1882.
[23] R. Benz and P. Läuger, Biochim. Biophys. Acta 468 (1977) 245.
[24] R. Benz and K. Janko, Biochim. Biophys. Acta 455 (1976) 721.
[25] G. Doetsch, Einführung in Theorie und Anwendung der Laplace-Transformationen, 3rd ed. (Birkhäuser, Basel, 1976) p. 169.
[26] E.T. Whittaker and G.N. Watson, A course of modern analysis, 4th ed. (University Press, Cambridge, 1965) p. 111.